A COMPARISON OF SYMMETRIC AND NON-SYMMETRIC LOADING ON PERFORMANCE OF BUCKLING-RESTRAINED BRACES

B. W. Saxey[1]

ABSTRACT

Buckling-Restrained Braces (BRB) are becoming increasingly popular in modern design, due to their high ductility and energy dissipation as well as their stable, predictable nature. Since their introduction into US building codes and recommended procedures, the BRB prequalification testing protocol have consisted of a symmetric loading history with incremental peak axial deformations increasing from the brace yield point to a displacement corresponding to, at least, the expected deformations of the structure. Symmetric loading protocols are sets of cycles with positive and negative amplitudes of equal magnitude which are then steadily increased, unlike actual earthquake demands which contain cycles of somewhat random amplitudes. Research and analysis has indicated that symmetric cycles may over-predict the peak brace force at a given level of deformation compared to that obtained from asymmetrical loading . This may be due in part to the increased cumulative strains that have built up prior to the larger symmetric cycles of the standard loading protocol of currently accepted building codes, as well as additional increases from isotropic hardening that may occur. This paper will examine multiple full-scale tests of BRB subjected to both symmetrical and non-symmetrical loading protocols and compare the resulting performance in terms of overstrength and cumulative inelastic ductility. Both pseudo-static and dynamic testing protocols will be examined.

Introduction

Buckling Restrained Braces (BRB) have seen increased use as lateral force resisting system elements. Use of the BRB element, and the determination of proper design factors, is often justified based on qualification tests performed according to testing requirements given in current building codes. These prequalification tests are commonly based on loading protocol comprised of symmetric cycles of increasing axial deformation. This type of loading protocol may not be representative of actual earthquake time histories and may not represent accurately the demands that will be put on the BRB nor the resulting overstrength generated. Earthquake loading would tend to be more random (asymmetric) in nature and would vary based on location. BRB testing performed to site-specific loading protocols are much less common due to their limited applicability at other locations and therefore, their higher economic cost when compared to their usability. However, limited testing has been performed and is a available for comparison.

This paper will compare the results of testing performed to a site-specific protocol with those performed to standardized symmetric loading protocol. Results will be compared primarily based on total brace force (brace overstrength) as well as measures of absorbed energy, and maximum achievable strain.

AISC BRB Prequalification Protocol Development

Early recommendations for BRB systems came from the 2001 AISC/SEAOC Recommended Provisions for BRB (AISC/SEOC 2001) and the 2003 NEHRP Recommended Provisions for New Buildings and Other Structures (FEMA 2003). Both of these documents recommended a loading protocol consisting of complete cycles (tension and compression steps in each cycle) of incrementally increasing symmetric displacements

---

[1]Chief Engineer, CoreBrace, West Jordan, Utah, USA 84047

beginning at the yield displacement (Δby) and increasing to a displacement corresponding to 1.5 times the design story drift (Δbm). Additional complete cycles were required to achieve a minimum cumulative inelastic ductility (CID) of at least 140 times the yield deformation. Specifically, the prequalification testing loading protocol was as follows:

(1) 6 cycles of loading at the deformation corresponding to Δby
(2) 4 cycles of loading at the deformation corresponding to 0.5Δbm
(3) 4 cycles of loading at the deformation corresponding to 1.0Δbm
(4) 2 cycles of loading at the deformation corresponding to 1.5Δbm

(5) Additional cycles of loading at the deformation corresponding to 1.0Δbm as required to reach a CID of 140.

As a minimum, 16 complete cycles would be required to qualify a BRB according to this protocol, each having an equal compression and tension step to the indicated ductility. The peak ductility requirement of 1.5Δbm and the CID requirement of 140 were based on a series of non-linear dynamic analysis performed as part of the NEHRP effort to produce its recommendations. This report states that the ductility capacity requirement represented a mean of response values and that the CID capacity requirement corresponded to the mean plus one standard deviation value. Equivalent elastic design procedures for Buckling Restrained Braced Frames (BRBF) at the time used a deflection amplification factor of either 5.0 or 5.5 for converting elastic deformations to inelastic deformations. Thus the BRB ductility requirement of 1.5Δbm represented an effective ductility requirement of at least 7.5Δby.

The 2005 AISC Seismic Provisions for Structural Steel Buildings (AISC 2005) increased the peak ductility requirement to 2.0Δbm as well as the CID requirement to 200. The distribution of intermediate steps and magnitude of the additional cycles to achieve the minimum CID were also adjusted. From these provisions, the prequalification loading protocol is as follows:

(1) 2 cycles of loading at the deformation corresponding to Δby
(2) 2 cycles of loading at the deformation corresponding to 0.5Δbm
(3) 2 cycles of loading at the deformation corresponding to 1.0Δbm
(4) 2 cycles of loading at the deformation corresponding to 1.5Δbm
(5) 2 cycles of loading at the deformation corresponding to 2.0Δbm

(6) Additional cycles of loading at the deformation corresponding to 1.5Δbm as required to reach a CID of 200.

A minimum of 10 complete cycles are required by the 2005 AISC Seismic Provisions with an effective ductility of at least 10Δby. These provisions also required that the deformation quantity, Δbm, be equal to the displacement corresponding to at least 1.0% story drift thus resulting in a peak deformation requirement corresponding to at least 2.0% story drift. This loading protocol remains unchanged in the 2010 AISC Seismic Provisions for Steel Buildings (AISC 2010). The time history of the AISC 2005/2010 loading protocol, showing a case where 2 additional cycles were required to achieve a CID of 200, is shown in Fig. 1.

It can be seen from Fig. 1 that the time-history indicated by the 2005/2010 prequalification protocol may not be representative of that of an actual event. Complete cycles consisting of compressive strains immediately followed by equal-magnitude tensile strains are likely not representative of what would be produced by a seismic event where asymmetric displacements would more likely be expected. A potentially more representative time-history is shown in Fig. 2. This loading history corresponds to a near-fault loading protocol developed by Lanning et al. (2013) as part of research investigating the use of BRB on long-span bridges.

Analyzing Cyclic Loading of BRB

When the loading protocol of the 2005/2010 AISC Seismic Provisions is applied, a BRB that experiences a tensile strain in the yielding core would have experienced immediately prior an equal magnitude compressive strain, resulting in a total cyclic strain of twice the peak strain value of the cycle as shown in Fig. 3. For example, a cycle resulting in a 2.5% tensile core strain would have been preceded immediately by a 2.5% compressive strain. The total cyclic strain experienced by the yielding core of the BRB would be twice this value, or 5%. Thus, the BRB subjected to the cyclic AISC protocol will experience cyclic strains equal to twice the peak cyclic value whereas a BRB subjected to an actual seismic event would likely undergo a total strain less than twice the peak value as it would be unlikely for loading to a particular deformation to have been preceded, or followed, by a deformation of exactly equal magnitude in the opposite direction.
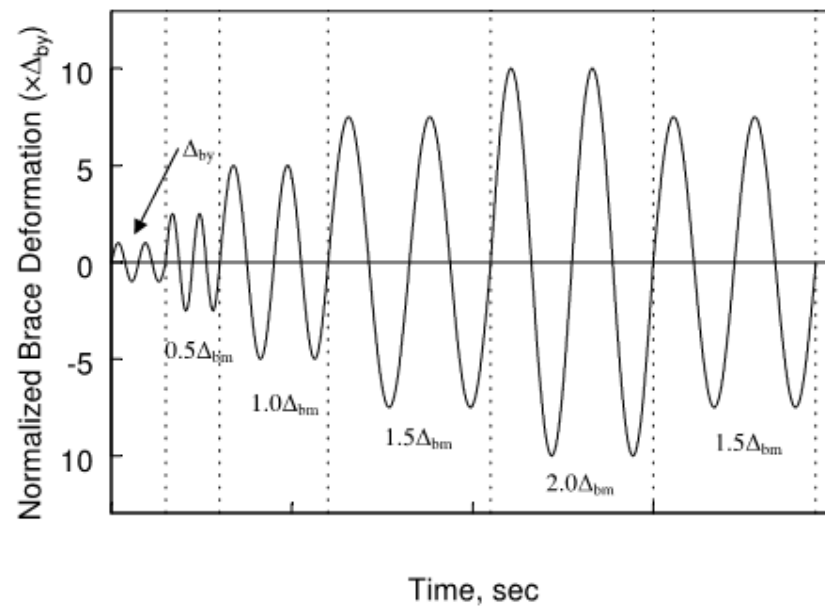
Figure 1.   Time-history representation of loading requirements of 2005 AISC Seismic Provisions.
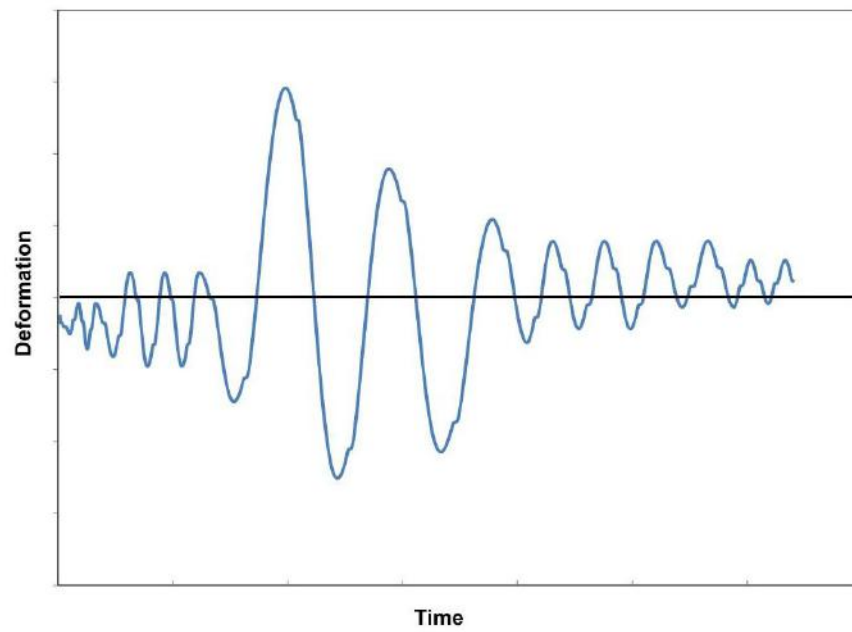

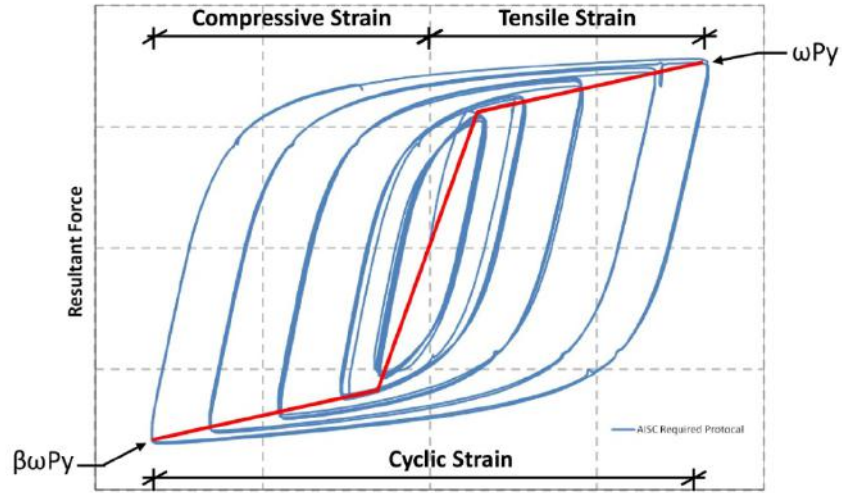Figure 2.   Time-history representation of asymmetric loading.

Figure 3.   Cyclic loading strain.

Recorded force versus displacement behavior from testing is often used to form a cyclic backbone curve, such as the one shown in red in Fig. 3. The cyclic backbone curve is made by connecting points of peak deformations and corresponding peak forces of representative cycles. For ease of comparison among tests of different BRB, peak brace displacements are usually referred to in terms of strain within the yielding core region. Similarly, peak brace forces are usually analyzed in a normalized form, with reference to the brace yield force as follows:

$$Puc = \omega\beta Py \tag{1}$$
$$Put = \omega Py \tag{2}$$

where Puc and Put are the peak compressive and tensile forces respectively, ω is the strain hardening adjustment factor, and β is the compression strength adjustment factor. The factors ω and β are referred to collectively as BRB overstrength factors. From rearrangement of Eqs. 1 and 2, it can be seen that ω is simply the ratio of the peak tensile force to the yield force and β is the ratio of the peak compressive force to the peak tensile force. These two expressions are written as,

$$\omega = Put/Py \tag{3}$$
$$\beta = Puc/Put \tag{4}$$

Qualification tests of BRBs with peak compressive forces less than peak tensile forces, at equivalent levels of deformation, do not meet the prequalification requirements of AISC 2005/2010. In other words, $\beta<1.0$ or $\omega\beta<\omega$ do not represent valid prequalification tests of BRB when based on the requirements of AISC 2010/2005.

The definition of β given in Eq. 4 is the traditional equation for β and only valid for symmetric loading where Put and Puc are measured at subsequent equal magnitude tension and compression deformations, respectively, within a cycle. Measuring β in this manner becomes mostly impossible for asymmetric loading since subsequent peak deformations are not typically of equal magnitude, nor do they necessarily result in a net change in state between tension and compression. Thus, the ratio of peak compression to peak tension from adjacent cycles provides little information on the behavior of the BRB under asymmetrical loading.

While the β term is difficult, if not impossible, to determine for asymmetrical loading, the $\omega\beta$ term, which together represents the total factor on yield force to equal peak compressive force, can be readily determined as follows,

$$\omega\beta = Puc/Py \tag{5}$$

Thus, at each peak cycle, regardless of symmetry, the overstrength factor for tension and the combined overstrength factor for compression can be represented by Eqs. 3 and 5 respectively.

Measuring peak brace forces from symmetrical testing protocol may result in amplified values when compared with the reference (compressive or tensile) strain at which the peak force was measured versus

the peak force that would be measured from an asymmetrical loading protocol at the same reference strain. With each excursion of a symmetric loading history, such as shown in Fig. 3, the brace undergoes a large net cyclic strain of twice that of the peak reference value at which it begins (or ends). For example, a symmetric loading that begins at a 3% compressive strain and continues to 3% tension strain has undergone a total cyclic strain of 6% and the material has strain hardened over this amount. Values for the peak force are reported, however, at the reference strain associated with the peak deformation relative to the un-deformed state, 3% in this case. Compare to an asymmetric loading cycle beginning at 0% strain and loading to 3% strain. This specimen would only strain harden over 3% strain and this value of overstrength would be reported at this 3% strain, but only half the strain hardening deformation would have taken place as in the symmetric example. The effect of this can be seen in Fig. 3 where the rate of strain hardening (or slope of the line) of the backbone curve shown in red, occurs at a greater pace than that of the actual measured strain hardening of the BRB shown in blue. Within an asymmetrical loading history there is no relationship between the cyclic strain and the reference strain. Thus the relative amounts of strain hardening at given reference strains can be greatly different between symmetric and asymmetric loading histories and measured overstrength will include more total strain hardening for symmetric loading at a given reference strain than will exist for asymmetric loading at the same reference strain.

Asymmetrical Testing

To investigate the effects of asymmetrical loading and in an effort to develop loading protocol for near-fault ground motions, Lanning et al. (2013) developed near-fault loading protocols shown in Fig. 4. The "proof protocol" considers a single site-specific design-level earthquake, while a generic, more demanding, "near-fault" protocol represents demands obtained from a suite of 18 scaled near-fault records. As seen in Fig. 4, a core strain of 5% is required in the testing protocols. The "proof protocol" was determined to be a good representation of the expected site-specific ground motions for the considered structure (Los Angeles, California, USA). The near-fault protocol is more rigorous in terms of number of excursions, containing nearly twice the total amount, and in terms of the number of high amplitude cycles. As shown in Fig. 4, both protocols have the peak strain shown in the positive (tensile) direction. The protocol can also be inverted resulting in a maximum strain with the brace in compression. These two options of peak strain in tension or compression are denoted hereafter with a -T or a -C after the protocol name respectively. (Such notation is not required for AISC protocols where a peak strain in one direction is always matched by an equal magnitude peak strain in the opposite direction.)

Testing was performed on two BRB to combinations of the loading protocol shown in Fig. 4. The two specimens, numbered 5 and 6, and had yield forces of 2947 kN (662 kip) and 1459 kN (328 kip) respectively. The applied protocol, testing rate, core plate configuration and other information relative to specimens 5 and 6 is given in Table 1. Of particular note from Table 1 is that core plate material was grade ASTM A36 (Fy 250 MPa, 36 ksi), that loading was performed at both dynamic and pseudo-static loading rates, and that each BRB was subjected to at least 2 full loading protocol successfully to completion. Specimen 6, as noted in Table 1, was also subjected to the AISC loading protocol in Fig. 1. Core fracture of specimen 6 occurred on the 10th cycle (final cycle) of the AISC protocol. The core of specimen 5 was not fractured.

The core plates of specimen 5 and 6 were cruciform (+) and flat (-) respectively. Schematic views of these specimens are given in Fig 5. Material grades for casings, stiffeners, connection plates and other relative items are also shown in Fig. 5.
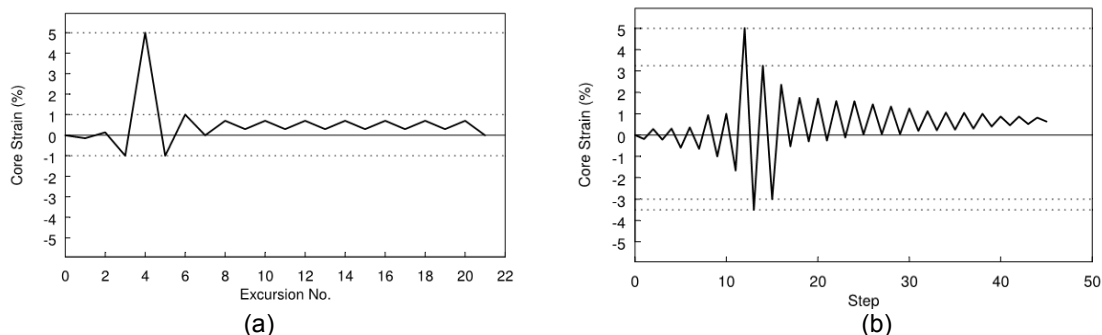

Figure 4.   Near-fault loading protocols (Lanning et al.): (a) proof protocol and (b) near-fault protocol

Table 1 Specimen Information

Specimen No.	Py (kN)	Core Plate		Extension Shape[c]	Loading Rate[d]	Tested Protocol Sequence		
		Steel Grade[a]	Shape[b]			1st	2nd	3rd
5	2947	A36	+	+	PS	Near Fault-T	Near Fault-C	n/a
6	1459		–	+	D	Proof-C	Near Fault-C	AISC[e]

[a] ASTM A36 steel grade nominal yield stress, Fy = 250 MPa
[b] (+) and (–) designate cruciform and flat plate cross-section, respectively
[c] All specimen have (+) shaped configuration beyond yielding core region
[d] "PS" and "D" designate pseudo-static and dynamic loading rates, respectively
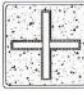[e] Fracture occurred
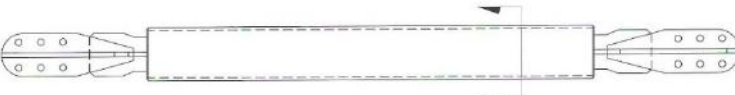
Figure 5.   Flat and cruciform representations of bolted BRB (CoreBrace)

**Comparison of Testing**

Time history displacement plots and resulting force displacement (hysteresis) plots of the tests of specimen 5 and 6 are shown in Figs. 6 and 7 respectively. For clarity, selected corresponding points from the time history plot and the hysteresis plots have been marked with alphabetic pointers by Lanning. Specimen 5 and 6 achieved CID values of 747 and 732 respectively. These high CID values (over 3 times the current AISC requirements) in combination with the high maximum strains, indicate good performance of the BRB. A resultant plot of normalized force (Pu/Py) in the braces as a function of core strain is shown in Fig. 8. The normalized force values shown in this figure are the values of ω and ωβ determined from Eqs. 3 and 5 respectively. Values of ω are shown in the first quadrant while values of ωβ are shown in the third quadrant as they both would be plotted on a standard force-displacement diagram with tension forces and strains being positive and compression forces and strains negative. Also shown in Fig. 8, for comparison, are the 70% prediction intervals determined by Saxey and Daniels (2014), which approximate a mean+1 standard deviation upper bound on the data reviewed. For ω plots, these prediction intervals were calculated for all connection types combined. For ωβ values the prediction intervals were calculated separately for individual connection types and for all connection types combined because the data showed such a separation. Fig. 8 shows the prediction intervals for ωβ values for both the bolted connection types and for all connection types combined. It can be seen that the prediction intervals for both ω and ωβ fairly accurately represent the data from the asymmetrical tests, although some ω values, at low strains in particular, are under-predicted.

From Fig. 8 it can be seen that there is general agreement between the resultant values of ω and ωβ between Specimen 5 and Specimen 6, which have (+) and (-) core plates respectively. It should be noted, however, that both of the specimens have a cruciform profile (+) at the non-yielding regions beyond the
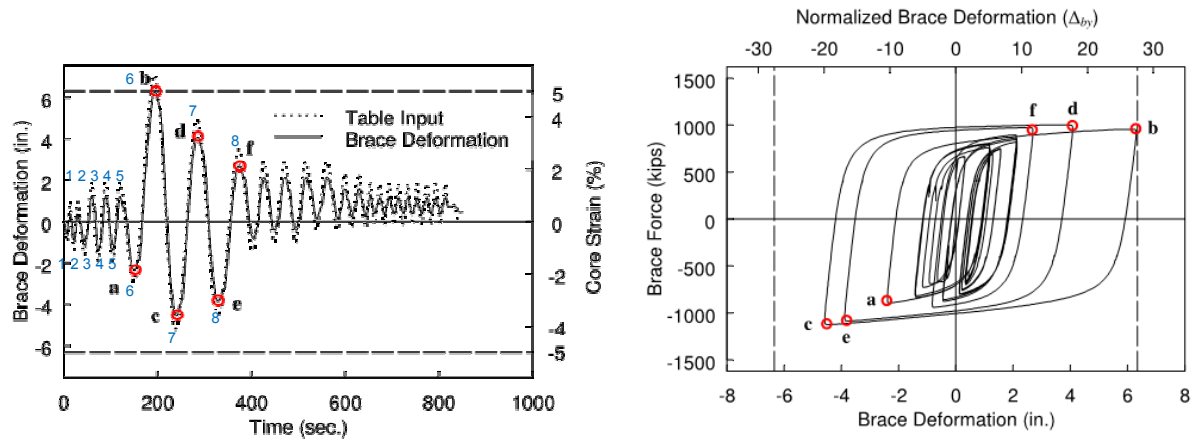
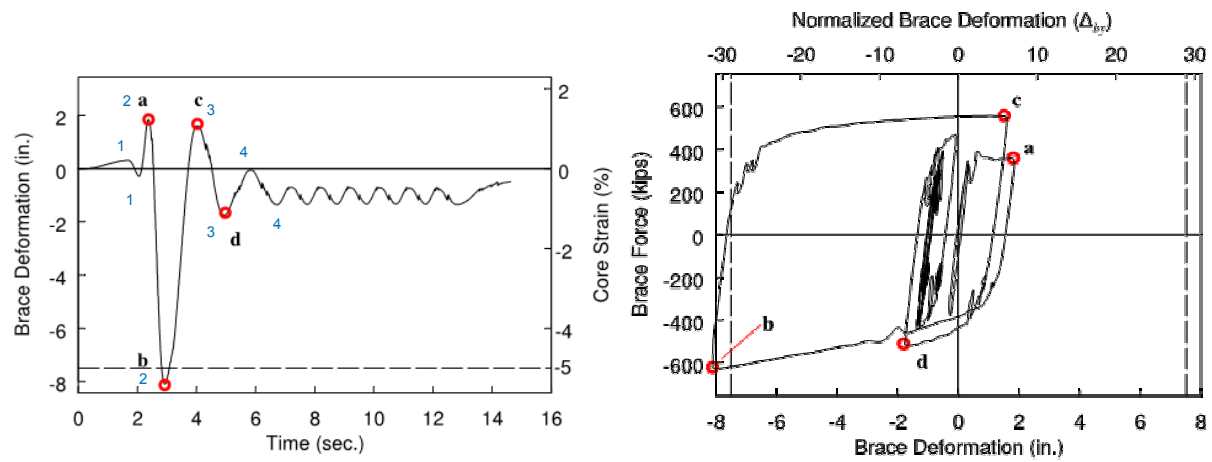(a) Specimen 5 Near Fault Tension Protocol (NFT)
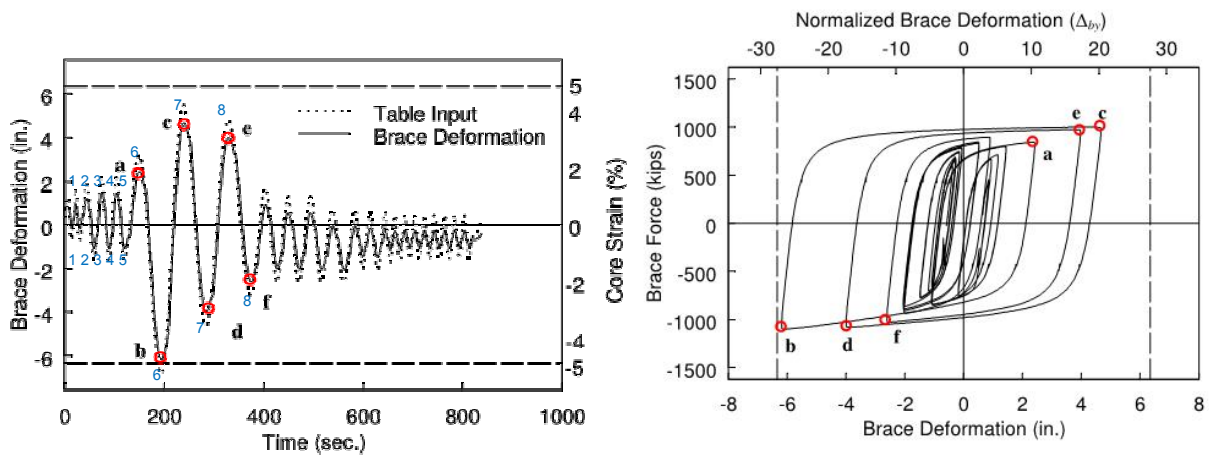
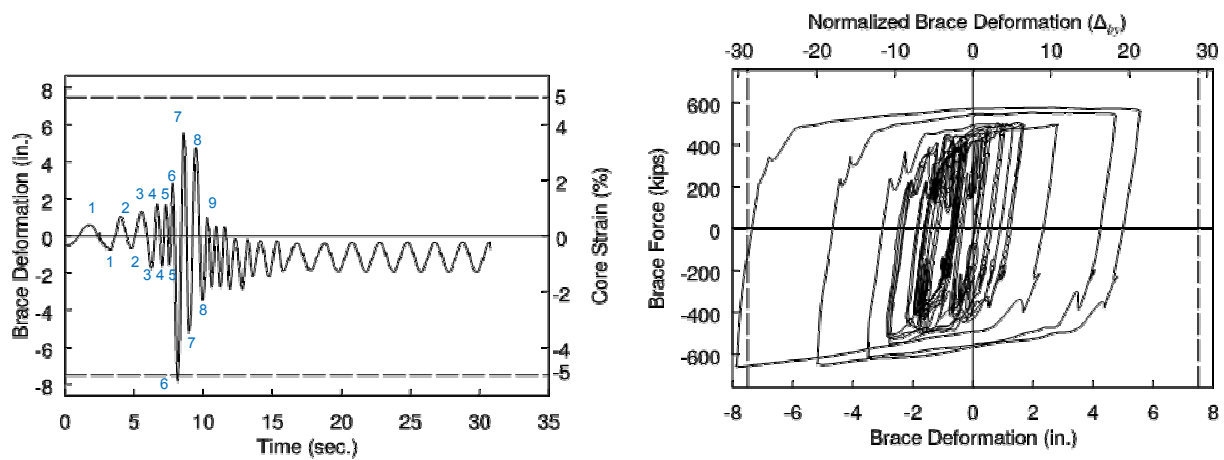
(b) Specimen 5 Near Fault Compression Protocol (NFC)

Figure 6. Specimen 5 Time history and resultant force-displacement plots. (Lanning et al 2013)

yielding core and both cores are fabricated from the same grade material. Also notable in Fig. 8 is that Specimen 6, which had two primarily-compression protocols (Compression Proof and Near Fault Compression), shows increased (larger negative value) ωβ values than does Specimen 5 which has one primarily-tension protocol and one primarily-compression protocol. Specimen 6 also shows higher overstrength, in general, than specimen 5, primarily at the many low-level displacement cycles of the dynamic near fault compression test.

Saxey and Daniels (2014) reviewed data of similar BRBs for the purpose of determining characteristic overstrength factors among BRBs of various manufacture, connection type, etc. From the BRBs considered, several were comparable to Specimen 5 and 6 in terms of characteristics provided in Table 1, in that they had bolted connections, (+) shaped core extensions, (+) or (-) yielding core configurations, and had yielding core material of grade A36. BRBs from this study that were considered for comparison to Specimen 5 and 6 come from testing performed by Merritt, et al. (2003), Newell, et al. (2005a) and Newell, et al. (2005b) and consist of CoreBrace Series D, F, and G respectively. A summary of the brace configurations of the BRBs from these tests, similar to the data given for Specimen 5 and 6 (as given in Table 1), is provided in Table 2. The BRBs in Table 2 consist of 12 total specimen, 4 with (-) yielding core configuration and 8 with (+) yielding core configuration. All 12 specimen were subjected to symmetrical loading protocol exceeding either the FEMA or AISC protocol as indicated in Table 2 and will be referred to hereafter with a specimen number followed by the test series number (such as 1D being test specimen #1 from the CoreBrace D series test by Merritt, et all.) in contrast to the specimen 5 and 6 from the non-symmetrical loading protocol from Lanning's tests which are not given a series indicator. All the test specimen achieved CID values significantly greater than 200 with the lowest achieving 590 and the highest achieving 1400. (D Series specimen achieved between 590 and 1400, F Series between 632 and 759, and G Series specimen between 631 and 1143.)

(a) Specimen 6 Dynamic Compression Proof Protocol (CP)

(b) Specimen 6 Dynamic Compression Near Fault Protocol (NFC)
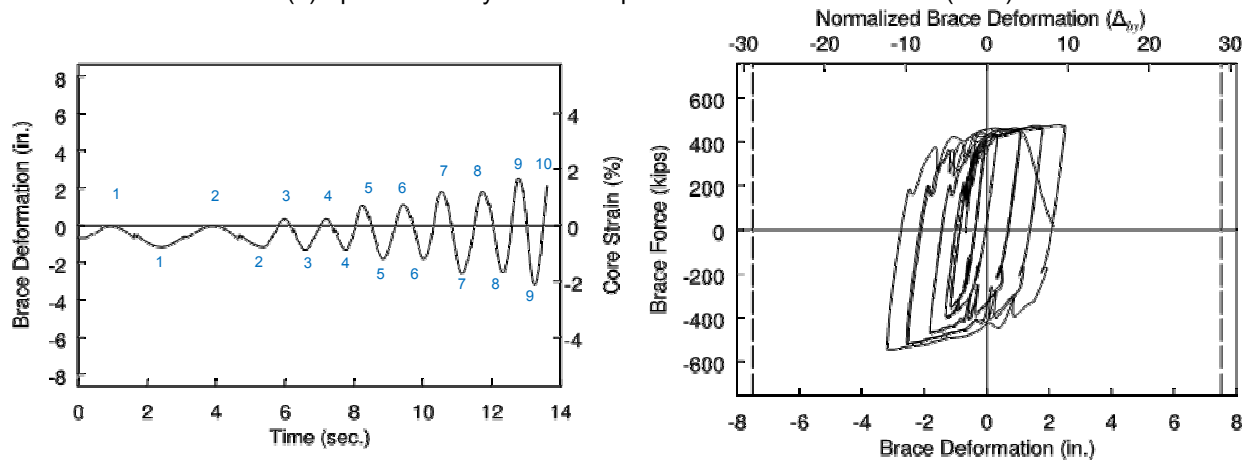
(c) Specimen 6 Dynamic AISC Protocol (A)

Figure 7. Specimen 6 Time history and resultant force-displacement plots. (Lanning et al 2013)
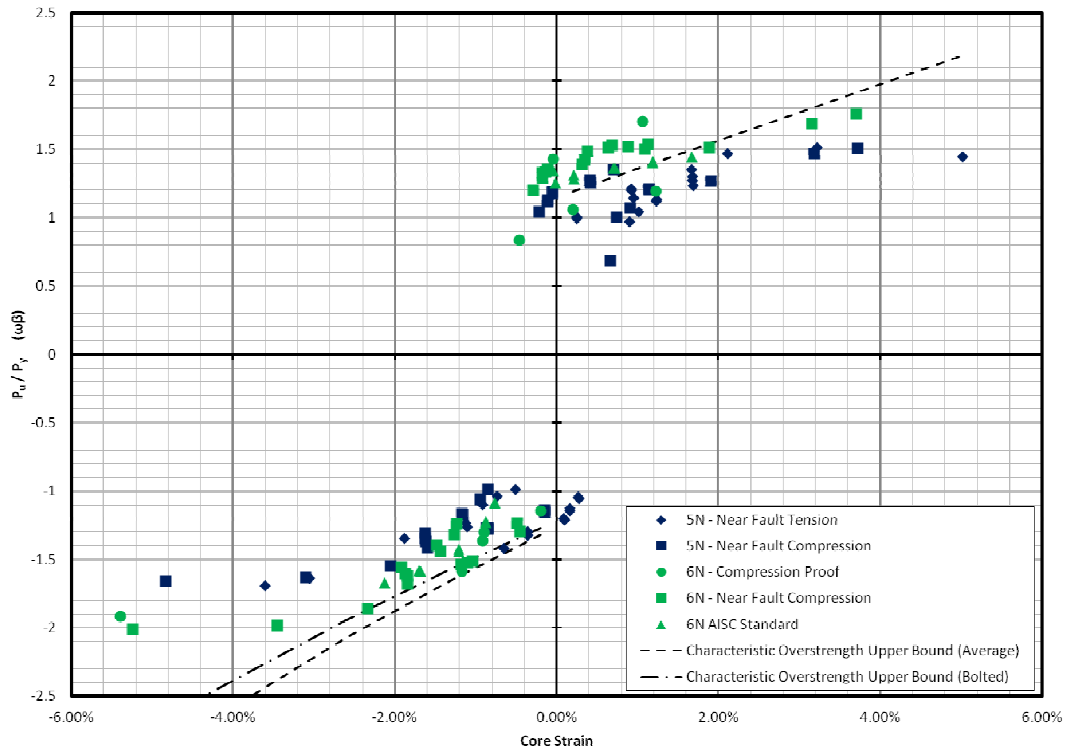
Figure 8. Specimen 5 & 6 resultant normalized force vs strain with characteristic 70% prediction intervals.

Table 2 Specimen Information

| Specimen No. | Py (kN) | Core Plate | | Extension Shape[c] | Loading Rate[d] | Tested Protocol Sequence | | |
		Steel Grade[a]	Shape[b]			1st[e,f,g]	2nd[h,i,j]	3rd[k,m]
1D	1723	A36	−	+	PS	SEOC/FEMA	HA-LCF	-
2D	1723		−	+	PS	SEOC/FEMA	HA-LCF	-
3D	3167		+	+	PS	SEOC/FEMA	HA-LCF	-
4D	3167		+	+	PS	SEOC/FEMA	HA-LCF	-
5D	3991		+	+	PS	SEOC/FEMA	HA-LCF	-
6D	3991		+	+	PS	SEOC/FEMA	HA-LCF	-
1F	4504		+	+	PS	AISC	AISC Ext1	HA
2F	4504		+	+	PS	AISC	AISC Ext1	
1G	2002		−	+	PS	AISC/FEMA	AISC Ext2	LCF
2G	2002		−	+	PS	AISC/FEMA	AISC Ext2	LCF
3G	4504		+	+	PS	AISC/FEMA	AISC Ext2	-
4G	4504		+	+	PS	AISC/FEMA	AISC Ext2	-

[a] ASTM A36 steel grade nominal yield stress, Fy = 250 MPa
[b] (+) and (−) designate cruciform and flat plate cross-section, respectively
[c] All specimen have (+) shaped configuration beyond yielding core region
[d] "PS" designates pseudo-static loading
[e] "SEOC/FEMA" protocol consists of cycles as follows: 6 at 1.0Δby, 4 at 2.5Δby, 4 at 5.0Δby, 4 at 7.5Δby, 2 at 10.0Δby, 4 at 15.0Δby
[f] "AISC" protocol consists of cycles as follows: 2 at 1.0Δby, 2 at 2.5Δby, 2 at 5.0Δby, 2 at 7.5Δby, 2 at 10.0Δby
[g] "AISC/FEMA" protocol consists of cycles as follows: 6 at 1.0Δby, 2 at 2.5Δby, 2 at 5.0Δby, 2 at 7.5Δby, 2 at10.0Δby
[h] "HA-LCF" denotes High-Amplitude Low Cycle Fatigue which consists of cycles at 15-20Δby until fracture
[i] "AISC Extended1" protocol consists of cycles as follows: 2 at 12.5Δby, 2 at 15.0Δby, 2 at 17.5Δby, 2 at 20.0Δby
[j] "AISC Extended2" protocol consists of cycles as follows: 2 at 12.5Δby, 2 at 15.0Δby, 2 at 18.5Δby, 2 at 21.5Δby
[k] "HA" indicates High Amplitude protocol consisting of 2 cycles at 20.0Δby
[m] "LCF" denotes Low Cycle Fatigue protocol which consists of 15 cycles at 15.0Δby

Specimen 3D-6D, 1F, 2F, 3G, & 4G have (+) core shapes similar to Specimen 5. Specimen 1D, 2D, 1G, & 2G have (-) core shapes, which is similar to Specimen 6. Test results of these two groups of test specimens, based on core shape similarity, are shown in Fig. 9 and 10 for (+) and (-) core shapes respectively. Fig. 9(a) shows results for ω for (+) core specimen and Fig. 9(b) shows results for ωβ for the (+) specimen. For simplicity, compressive core strains and resulting ωβ values have been formatted to show in the first quadrant and give positive values of ωβ for positive values of strain. Fig. 10(a) and 10(b), similarly show ω and ωβ comparisons for the (-) specimen. For plots showing ω, the tension peaks shown in Figs 6 and 7 have been numbered for each protocol (as seen in Figs. 9 and 10) and are shown, along with a prefix containing the protocol abbreviation, as data labels for the points in Figs. 9 and 10. For example, the point labeled (d) Fig 6(a) is the 7th tension peak for Specimen 5 in the Near Fault Tension (NFT) protocol. As such, this point is labeled NFT7 in Fig. 9(a). Since this point is also specifically labeled in Fig 6(a), as point d, the label in Fig. 9(a) is appended to include this extra identifier as NFT7 (d). Peaks from Figs 6 and 7 that aren't specifically labeled with an identifier are only labeled with the protocol abbreviation and peak number. For reference among these sets of figures, the first several peaks of the protocol in Figs. 6 and 7 have been labeled. This numbering is useful for observing the order in which the reported data point occurred in the test protocol and how it compares to values from other places in the testing. Points from the Specimen 5 and 6 tests which are at negative strains or which result in overstrength values of less than 0.8 have been omitted from Figs. 9 and 10. These points result from small displacements that do not exhibit a net change in the state of compression or tension and are considered inconsequential. The omitted points can still be seen in Fig. 8. It should be noted that a test that is primarily compressive, such as the Near-Fault Compression (NFC) protocol, still has tension peaks. As such, the ω values resulting from these peak readings are given on the ω plots of results. The resulting plot of ω values will have points from primarily tension and compression protocols (such as NFT6 and NFC9) but both sets of values are measurements of peak tension readings regardless of the protocol they result from. The same has also been done for ωβ plots with the compressive peaks numbered sequentially for reference. Plotted values exist on these plots from primarily compression protocols and primarily tension protocols, but both sets of data are measurements of compressive peaks and both give ωβ values regardless of the series name.

It can be seen from Figs 9(a) that nearly all the resultant ω points would be conservatively predicted from the symmetrical protocols of the D, F, and G series tests. While a few points, such as NFC9, 10, and 11, do fall above the lines of D, F, and G series results, they are at small strains from late in the protocol at cycles that had residual deformation and had little, if any, change of compressive or tensile state. The points of high strain fall at or below the values that would be expected based on the results of the D, F, and D series symmetric tests. Point NFT6(b), in particular, falls well below the value that would be predicted from even the lowest ω overstrength curves of the 3D and 4D specimen. It is also noteworthy that point NFT6(b) shows a lower overstrength (1.44) at just over 5.0% core strain than was measured at point NFT7(d) (1.51) at a smaller core strain of just over 3.2%. Examination of Fig 6(a) shows that while the reference tensile strain of point (b) (at just over 5.0%) is indeed greater than that of point (d), point (a) is a much smaller compressive strain (around 1.9%) than is point c (around 3.6% strain). As such the total cyclic strain from point (a) to (b), which is about 5.0-(-1.9) = 6.9%, is nearly identical to the total cyclic strain from point (c) to (d) of 3.2-(-3.6) = 6.8%. Either of these two sets of points would have a total cyclic strain (from peak compression to peak tension or vice versa) equal to the total cyclic strain of a symmetric test of about 6.8%/2 = 3.4% which is very near the strain of point NFT7(d) on Fig. 9(a) which has an overstrength of what would be expected by extrapolating the 3D and 4D curves to a strain of 3.4%. The cycle from (c) to (d) on the Specimen 5 NFT test is nearly symmetric and produces an ω value of what would be expected by extrapolating the symmetric test results of 3D and 4D. The cycle from (a) to (b), with nearly the same cyclic strain, does result in a measurably lower overstrength value of ω than occurs from (c) to (d). The additional overstrength measured at point (d) (1.51) versus point (b) (1.44) is likely due to the cumulative effects of loading at a second cycle of high amplitude and the resulting isotropic hardening.

Fig. 9(b) shows very similar results for measured values of ωβ of the (+) core shaped specimen as is seen in Fig. 9(a) for ω. Nearly all measurements of ωβ fall below the results of the symmetric testing. Large compressive strains, such as that at NFC6(b) result in smaller ωβ values than would be expected by extrapolating the symmetrical test backbone curves. Points NFC6(b) and NFC7(d) also have nearly the same measured value of ωβ even though the reference compressive strain of point NFC6(b) is considerably higher than NFC7(a). However, when considering the cyclic strain from tension to compression, both points are the results of a cyclic strain of about 6.8%. Dividing this value in half, 3.4%, and comparing to the extrapolation of the 3D and 4D test results, an ωβ value of around 1.68% would be expected, which is very similar to the value of NFC6(b) and NFC7(d). As with the ω values, the total cyclic strain seems to be a reasonable predictor of overstrength for high level strains of non-symmetrical loading.

Examination of Figure 10(a), which compares resultant values of ω for the (-) core shaped specimen, shows several readings for the non-symmetric loading protocol that exceed those from the symmetric loading
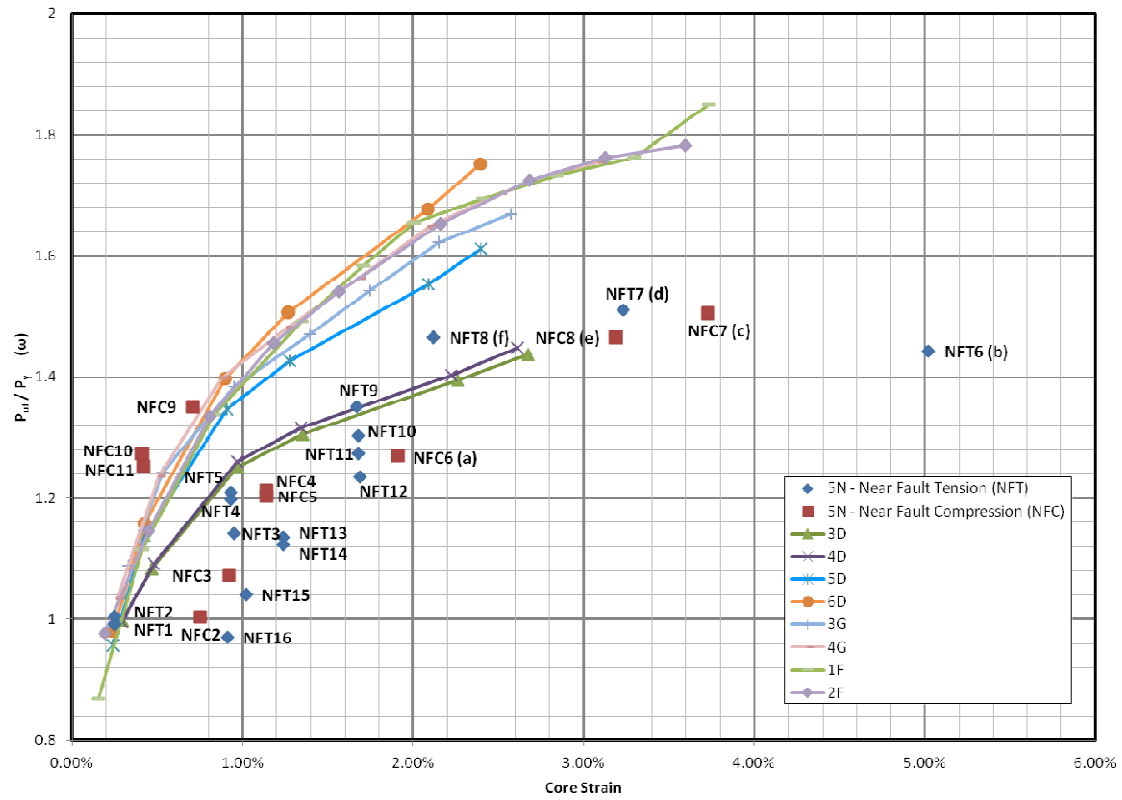
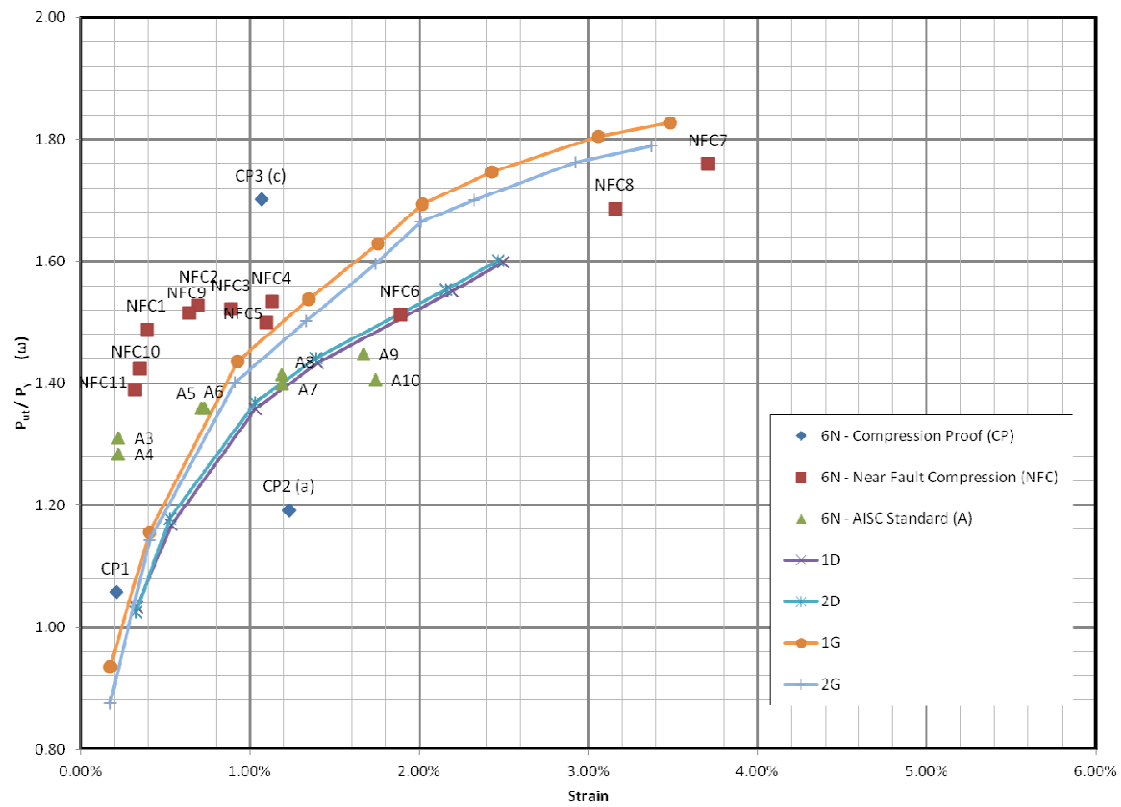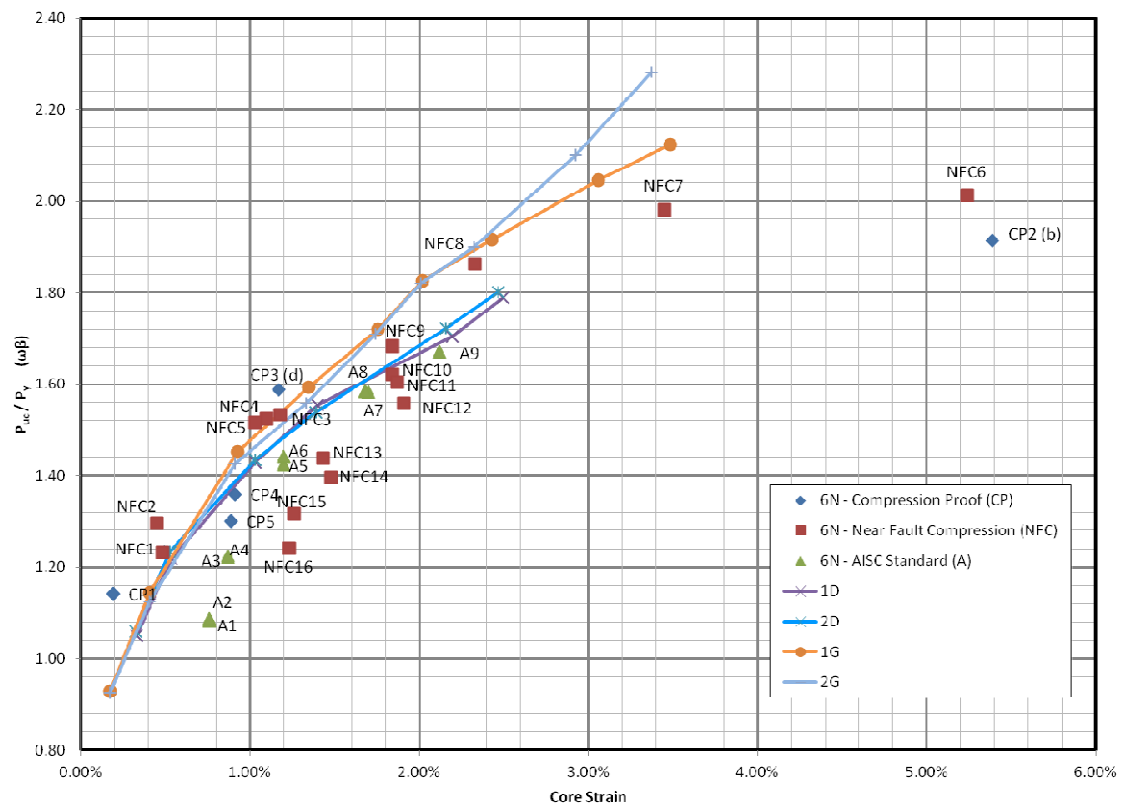(a) Strain Hardening Overstrength, ω
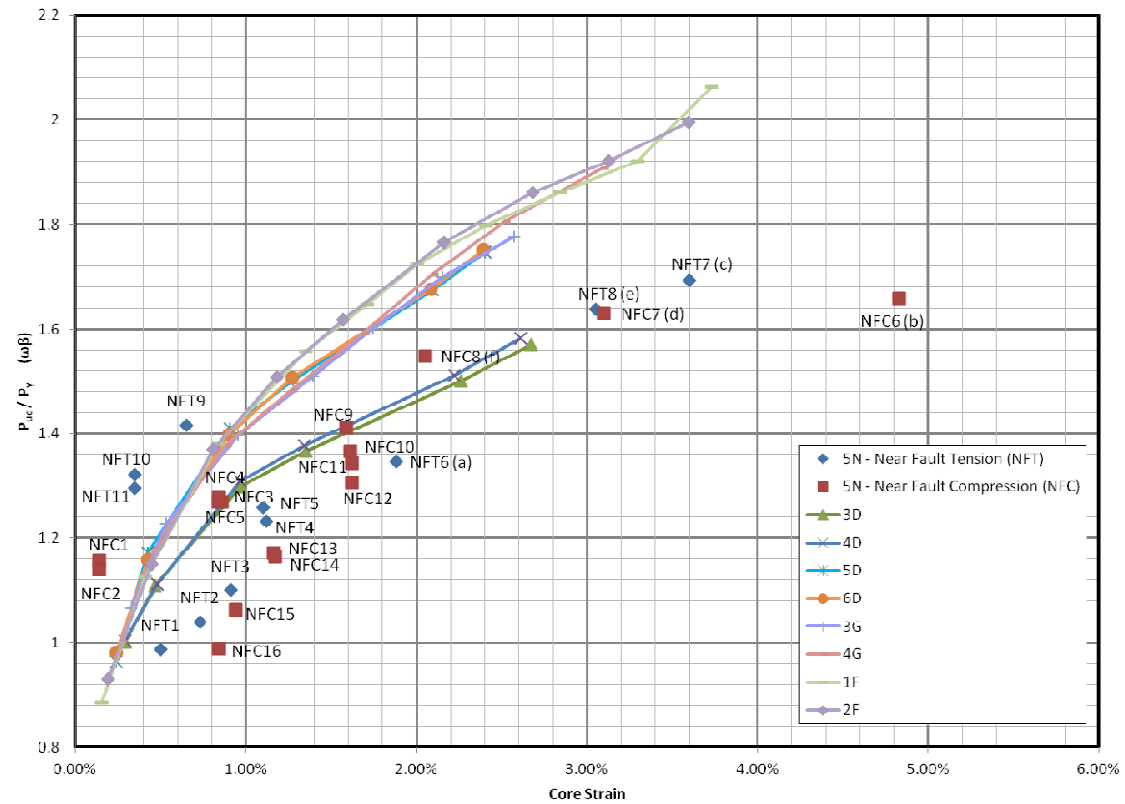
(b) Compression Overstrength Factor (ωβ)

Figure 9. Comparative normalized force vs strain for (+) core shapes.

(a) Strain Hardening Overstrength, ω

(b) Compression Overstrength Factor (ωβ)

Figure 10. Comparative normalized force vs strain for (-) core shapes.

protocol of 1D, 2D, 1G, and 2G. However, many of these points are from the very small cycles of the Near Fault Compression (NFC) protocol such as NFC1-5 and NFC9 and greater. These NFC cycles are very small are occurring after the Compression Proof (CP) has occurred which had already introduced considerable strain hardening into the core material. Indeed, the values of NFC1-6 all result in nearly the same value of ω even though the strain levels vary from less than 0.5% to nearly 1.9% indicating a pre-existing level of strain hardening. These cycles are nearly symmetric and as such, the value of total cyclic strain is nearly twice the value of the reference tension strain. Points NFC9-11 are also nearly symmetric, but are offset from the point of zero deformation. NFC9 from Fig. 10(a) is measured at a tensile strain of 0.64% with an ω value of 1.52. The immediately preceding compressive point (NFC8 from Fig. 10(b)) is measured at 2.33%. Thus the total reference strain is 0.64%-(-2.33) = 2.97% which would be comparable to a reference strain of 2.97/2 = 1.49% from a symmetric test. At 1.5% strain, the D and G series tests show in Fig. 10(a) would give ω values of about 1.45 and 1.55 respectively (taking the average of the 2 specimen in each series). Thus, the value of ω measured at point NFC9 fits right between the D and G series test results at the similar level of total cyclic strain and the value of the ω at point NFC9 is as would be expected. Cycles after NFC9 are slightly smaller in total cyclic strain and the resulting ω of NFC10 and 11 show as much. Cycles after NFC 11 result in a negative tensile strain since they never experience net tension and are omitted from Fig. 10(a).

Points NFC7 and NFC8 on Fig. 10(a) are measured at reference strains of 3.71% and 3.16% respectively, and the resulting measurements of ω fall nicely between the values the D and G series symmetrical tests. The cycles at this point in the NFC protocol are also nearly symmetrical and as such the results are expected. The compressive peak immediately before the large tensile peak associated with NFC 7 is the large compressive point NFC6 from the ωβ plot shown in Fig. 10(b). The ωβ NFC6 point is taken at a compressive strain of 5.24%. Thus the total cyclic strain between the compressive peak NFC6 and the tensile peak NFC7 is 3.71-(-5.24) = 8.95%, which could be compared to a reference strain of a symmetric test of 8.95/2 = 4.48%. Examination of the plots on Fig. 10(a) would suggest that extrapolating either the D series or the G series tests to this level of strain would result in an ω value of around 1.88, higher than measured at point NFC7. A similar exercise for NFC8 gives a total cyclic strain of 3.16-(-3.45) = 6.61% suggesting comparison at a reference strain of 6.61/2 = 3.30%. This is very nearly the actual reference strain of NFC8 (indicating that the cycle is very nearly symmetric) and as such, it's ω measurement is nearly what would be expected from the D series tests and less than that expected from the G series tests.

As a comparison, the data for the CP, NFC, and AISC protocols have been adjusted to show the equivalent reference strain in Fig. 11, rather than the actual reference strain that is used to plot the points in Fig. 10(a). This was done by taking the average of the strain at the peak tension displacement and the strain of the immediately preceding peak compression displacement (using absolute values) and dividing the result in half as described above. The resultant plot shows the same values of ω as Fig. 10(a) but at the equivalent reference tension strain rather than at the measured reference strain. Fig. 11 confirms that the data is well represented by the symmetric tests of the D and G series when it is plotted at the equivalent reference strain although some values, particularly at low strain levels, remain higher than what would be predicted by the symmetrical testing.

A final examination of the compressive measurements for the (-) shaped core specimen shows that the results given in Fig 10(b) are very similar to those for the (+) shaped specimen shown in Fig. 9(b). The points NFC6 and NFC7 lie at values that would be expected from extrapolating the symmetrical test data. The point NFC6, similar to NFC6(b) on Fig. 9(b) for the (+) braces, is the product of more asymmetrical loading than NFC7 and has a higher reported reference compression strain. As such, its reading appears further to the right of Fig. 10(b) than does the result for point NFC7. However, points NFC6 and NFC7 are the results of nearly identical total cyclic strains of 7.13% and 7.16% respectively and as such it seems reasonable that they both have nearly identical values of ωβ. Dividing these cyclic strains in half to get a comparable reference strain of a symmetric test gives reference strain values of 3.57% and 3.58% for NFC7 and NFC7 respectively. This is nearly the reference strain level of NFC7 (indicating it consists of a nearly symmetric cycle), and the reported ωβ value for both NFC6 and NFC7 seems to be well predicted by the symmetric tests at this equivalent reference strain. Point CP2(b) on this same figure is also the result of a 5.39% compression strain that followed a 1.07% tension strain and has a reported ωβ value of 1.91 (at 5.39% reference strain). This point has a total cyclic strain of 6.62% and dividing this in half gives an equivalent reference strain of 3.31%. At this level of strain, the extrapolated D series tests would predict an ωβ value of around 2.0 and the G series tests would report a value of around 2.1. Again, the symmetric tests predict well the ωβ value of the asymmetric test at the equivalent reference strain.

The ωβ values of points NFC6 and NFC7 from the (-) tests as shown on Fig. 10(b) are notably higher than those of points NFC6(b) and NFT7(d) of the (+) tests from Fig. 9(b). While it is true that the the (-) tests for specimen 6 were dynamic and the (+) tests of specimen 5 were not, this factor is likely not the major cause
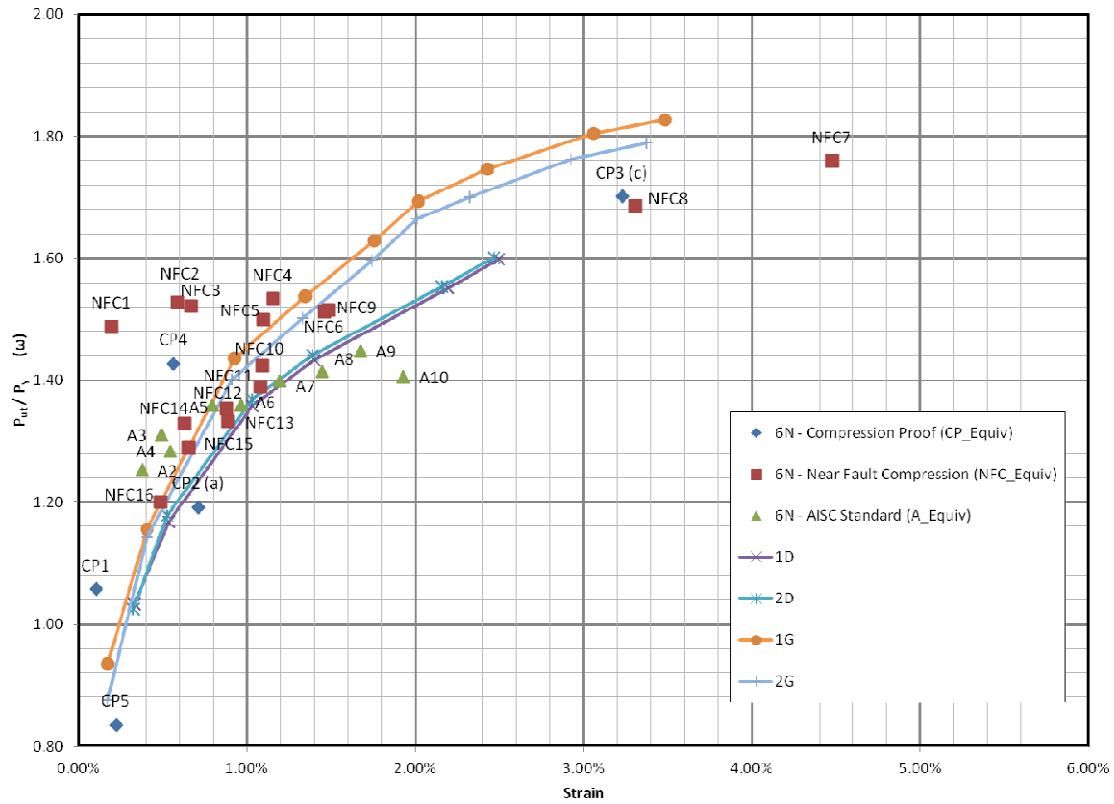
Figure 11. Comparative normalized force vs. strain at equivalent reference strains.

of the difference. It can be seen that both sets of asymmetrical tests (the dynamic 6N tests and the pseudo-static 5N tests) follow the symmetrical, pseudo-static test results, especially when considering equivalent reference strains as mentioned above, indicating that the dynamic loading does not cause unexpected performance. It is more likely that the combination of the (-) shape of the core and the fact that the (-) core specimen are all lower capacity braces is the cause of the higher $\omega\beta$ values seen in Fig. 10(b). The smaller capacity (-) braces would in general have lighter, more flexible connections and non-yielding regions than the higher capacity (+) braces would.

The AISC tests shown in both Fig. 10(a) and 10(b) show that for the first few cycles there remains an effect of the asymmetrical, high deformation protocol that immediately preceded it, but within a few cycles the behavior returns to match similarly the behavior of the symmetrical tests. It is also noteworthy that specimen 6 fractured at the 10th cycle of the AISC protocol (point A10 Fig 10(a)) at a reference strain of 1.74%. Considering the symmetric nature of the AISC protocol, this would be equal to a total cyclic strain of 2x1.74% = 3.48% strain. Both this reference strain, and the cyclic strain at fracture are considerably less than strains that this brace had already experienced in previous cycles. This indicates that CID, which had reached 733 in this brace, is a strong contributor to fracture performance of the BRB core. As such total durability, the combination of strain and accumulated inelastic ductility, must both be considered in determining the adequacy of tested braces for use in projects.

Conclusions

Asymmetrical loading histories result in overstrength values that may not be represented well by the results of standardized symmetric testing of BRB at the same reference strain. Asymmetrical loading generally results in lower overstrength values than comparative symmetric loading at the same reference strain, though some exceptions occur, particularly at low amplitude cycles that do not completely reverse. When the total cyclic strain is considered and the results of asymmetric testing are viewed at an equivalent reference strain, many of these exceptions are removed and a better correlation is observed with fewer values exceeding those from the standardized symmetrical testing. Cases do remain where symmetrical testing would considerably under predict the expected overstrength of asymmetrical loading histories. Fully reversing cycles seem to relieve this higher overstrength and return it to performance similar to measured overstrength from symmetrical testing. More research is needed to understand this phenomenon.

References

AISC/SEAOC, 2001, *Recommended Provisions for BRB*, Structural Engineers Association of California: Seismology and Structural Standards Committee and American Institute of Steel Construction, Inc.

FEMA 450, 2003, *NEHRP Recommended Provisions for New Buildings and Other Structures*, Building Seismic Safety Council for The Federal Emergency Management Agency, Washington D.C.

AISC, 2005, *341-05, Seismic Provisions for Steel Buildings*, American Institute of Steel Construction, Inc., Chicago.

AISC, 2010, *341-10, Seismic Provisions for Steel Buildings*, American Institute of Steel Construction, Inc., Chicago.

Lanning, J., Benzoni, G., Uang, C.M., 2013, *The feasibility of using buckling-restrained braces on long-span bridges: Near-fault loading protocols and full-scale testing* SSRP Report No. 13/17, Dept. of Structural Engineering, Univ. of California, San Diego, La Jolla, Calif.

Saxey B., Daniels M, 2014, *Characterization of Overstrength Factors for Buckling Restrained Braces*, Australasian Structural Engineering (ASEC) Conference, Auckland New Zealand July 9-11 2014

Merritt S., Uang C.M., Benzoni G., *2003, Subassemblage Testing of CoreBrace Buckling-Restrained Braces, Report No. TR-2003/01*, University of California, San Diego, CA. [CoreBrace D Series]

Newell J., Uang C.M., Benzoni G., *2005a, Subassemblage Testing of CoreBrace Buckling-Restrained Braces (F Series), Report No. TR-05/01*, University of California, San Diego, CA. [CoreBrace F Series]

Newell J., Uang C.M., Benzoni G., *2005b, Subassemblage Testing of CoreBrace Buckling-Restrained Braces (G Series), Report No. TR-06/01*, University of California, San Diego, CA. [CoreBrace G Series]